

# The VascuLens - A Handsfree Projector-Based Augmented Reality System for Surgical Guidance During DIEP Flap Harvest

Sebastian Gonzalez<sup>1</sup>, Michael J. Stein<sup>2</sup>, Robert Rohling<sup>1,3</sup>, Philip Edgcumbe<sup>4</sup>

<sup>1</sup>Electrical and Computer Engineering, University of British Columbia, Vancouver, Canada

<sup>2</sup>Department of Plastic Surgery, Lenox Hill Hospital, New York, United States of America

<sup>3</sup>Department of Mechanical Engineering, University of British Columbia, Vancouver, Canada

<sup>4</sup>Department of Radiology, University of British Columbia, Vancouver, Canada

**Abstract**— Augmented reality technologies are increasingly being used to provide enhanced surgical navigation for surgeons. The goal of such augmented reality technology is to improve both the safety and efficiency of operations. The VascuLens, a novel handsfree and focus free projector-based augmented reality system, is presented in this paper. The proposed application for the VascuLens is for improving visualization of the vascular anatomy during deep inferior epigastric perforator (DIEP) flap breast reconstruction. The DIEP flap is a fasciocutaneous flap that is harvested based on perforating vessels 1-2mm in size and then connected under the microscope to the internal mammary vessels in the chest to create a new breast mound after mastectomy. The ultimate goal of this work is that the VascuLens system will take preoperative CT scan data, register the preoperative data to the patient on the operating room table, and project the segmented DIEP arteries directly onto the patient. The novel aspects of the system include: 1) a handsfree projector, 2) a simple preoperative to intraoperative image registration technique that does not require a fiducial marker or camera, 3) and intraoperative surgeon-in-the-loop surgical guidance. This paper describes the proof-of-concept Vasculens workflow and reports the Vasculens accuracy. The accuracy is reported as a function of registration technique, patient body type, projector height and projector angle. Using the ideal registration technique, projector height and projector angle, the mean absolute point reprojection error is 1.7mm, making it a good candidate for DIEP flap breast reconstruction surgery.

**Keywords**— Augmented reality, vascular anatomy, intraoperative, DIEP flap harvest, mixed reality

## I. INTRODUCTION

Following a mastectomy, breast cancer patients commonly undergo breast reconstruction, either using alloplastic materials (implants) or autologous tissues (flaps). The most common form of autologous breast reconstruction to date is the deep inferior epigastric perforator flap (DIEP). This surgery involves harvesting abdominal skin and fat (supplied by perforators of the deep inferior epigastric artery and vein (DIEA/V) and connecting the vessels to the internal mammary artery and vein (IMA/V) under the costal cartilages of chest to create a breast mound.

The most time consuming and risk-prone step in this 8-hour surgery is the dissection of each perforator from the surrounding rectus abdominis muscle. This commonly involves the surgeon delicately separating the individual muscle fibers off the vessels as they follow the vessels proximally to their origins off the iliac arteries. As the surgeon visualizes different perforating vessels piercing the muscular fascia they also have to choose which perforators to harvest while sacrificing the least amount of muscle possible. This involves a certain degree of estimation of the trajectory and orientation of these vessels under the fascia.

To help plan the surgery and reduce injury during dissection, surgeons commonly order a CT angiogram preoperatively so that the radiologist can document, relative to the umbilicus, the location of each perforator artery as it pierces through the rectus fascia. The surgeon then uses the information provided by the radiologist to draw the location of the perforator arteries onto the patient (Figure 1). The error in drawing such markings is approximately 1 mm [1]. This error serves as the approximate reprojection error guideline for DIEP surgical guidance.



Figure 1: Picture of patient's abdomen prior to DIEP flap surgery. The crosses mark the locations of the DIEP arteries.

Plastic surgeons are increasingly focused on increasing the speed and safety of their dissection, most notably during intramuscular flap dissection, which usually represents the longest and most laborious aspect of flap harvest.

Recently, AR navigation guidance systems have been successfully used in urological [2, 3], extremity surgery [4],

and DIEP flap breast reconstruction. [5, 6]. In one instance, Microsoft HoloLens augmented reality glasses were used in a preoperative DIEP flap setting [5]. While effective, this technology is expensive, cumbersome to use intraoperatively and incompatible with the surgeon's headlamp and operative loupes. Furthermore, no accuracy data is reported. Another group created a combined handheld projector and camera device to project DIEP arteries and their intramuscular trajectories onto the patient [6]. Preoperative CT angiogram data was registered directly to the patient on the operating room table by placement of black-and-white markers on anatomical landmarks. The anatomical landmarks were the symphysis, umbilicus, and bilateral anterior superior iliac spines. Once the registration was complete, the assistant held the projector while the surgeon used a marking pen to trace and draw the projected information onto the patient. After the projector and black-and-white markers were removed, the surgery began. The extent of reporting about projection accuracy was that the authors noted that on a few occasions there was a systematic shift between preoperative and intraoperative perforators of  $> 1$  cm. This handheld projector was tested via a randomized, open, single-center, superiority trial with 60 patients undergoing DIEP flap breast reconstruction.

In contrast to the technologies described above, the Vasculens system is simple. It is a single projector with intuitive user operation that only requires clicking on marks in the surgical field. In spite of its simplicity, it offers surgeon-in-the-loop handsfree AR intraoperative guidance. Surgeon-in-the-loop refers to the ability of the surgeon to use the projected anatomy as a reference (or road map) while dissecting the vessels free from the surrounding muscle. With the anatomical knowledge of the perforator interconnectivity, the surgeon can speed or slow down their dissection accordingly. This new technology therefore has the potential for improving both safety and efficiency in the operating room.

## II. METHODS

### A) *Materials*

The Vasculens system includes the following hardware components: 1) a PicoPro laser projector (Cellulon, Seoul, Korea) with 1920 x 720p resolution and brightness of 32 lumens, 2) a mounting arm for holding the projector above the surgical scene, which for the experiments in this paper is a converted desk lamp with an adjustable suspension arm stand, 3) a laptop computer which can run the software and connect to the projector via HDMI cable.

The Vasculens system's main software components are: 1) IntelliSpace (Philips, Amsterdam, Netherlands), 2) the console application (C++ and OpenCV), and 3) OBS Studio [8], a third-party program which connects the console application to the projector.

### B) *Clinical and technical workflow of Vasculens*

The workflow of the Vasculens system is as follows:

#### **Step 1 - Generating the initial source image ( $P_{src}$ ) from the preoperative CT angiogram**

The radiologist uses Philips IntelliSpace software to view the preoperative CT angiogram and document the location of each perforator artery as it pierces through the rectus fascia as well as four points that will be used for registration. Next, the radiologist segments the DIE arteries. Finally, the radiologist generates the initial projector image ( $P_{src}$ ) by capturing a 2D image of the segmented anatomy, as seen from a camera height of 1.5 m above the umbilicus.

#### **Step 2 - Preoperative to intraoperative registration to generate the distorted destination projector image ( $P_{dst}$ ) :**

As shown in Figure 1 and described in the introduction, the surgeon draws crosses onto the skin of the abdomen to mark out the approximate locations where the perforator arteries pierce through the rectus fascia of the patient as well as four registration points. The Vasculens projector is placed above the patient's umbilicus and the surgeon uses a laser projected computer cursor to click on the four registration points ( $x_i'$  and  $y_i'$ ) that the surgeon recently drew onto the patient ( $x_i$  and  $y_i$ ). These points are at identifiable locations that relate to the perforator arteries. As shown in equation 1, these four corresponding points are then used to calculate the scaling factor ( $t_i$ ) and the 3x3 mapping matrix  $M$  by Gaussian elimination via the OpenCV *getPerspectiveTransform* function [7].

$$\begin{bmatrix} t_i x_i' \\ t_i y_i' \\ t_i \end{bmatrix} = M \cdot \begin{bmatrix} x_i \\ y_i \\ 1 \end{bmatrix} \quad (1)$$

Next, the OpenCV *warpPerspective* function [7] and the 3 x 3 matrix  $M$  are used to transform (translation, rotation, scaling, shear, reflection)  $P_{src}$  into  $P_{dst}$ . This is shown in Eqn. 2. and the final projection of  $P_{dst}$  onto the patient or mannequin is shown in Figure 4.

$$P_{dst}(x, y) = P_{src} \left( \frac{M_{11}x + M_{12}y + M_{13}}{M_{31}x + M_{32}y + M_{33}}, \frac{M_{21}x + M_{22}y + M_{23}}{M_{31}x + M_{32}y + M_{33}} \right) \quad (2)$$

**Step 3 - Intraoperative guidance:**

With  $P_{dst}$  continuously projected onto the patient and showing the location of relevant vascular anatomy, the surgeon can dissect the abdominal skin, locate the perforator arteries, and proceed with the 6-8 cm intramuscular DIE arteries.

*C) Experimental Data Collection*

Experimental data was collected, first in a controlled environment to assess fundamental accuracy limits, as follows: To simulate a patient and a CT scan snapshot from Philips IntelliSpace, a picture was taken with a A51 Samsung 48MP digital camera (Seoul, South Korea) of a mannequin with a 8 x 9 checkerboard taped onto its abdomen. Using a custom corner detector, the coordinates ( $x_i$  and  $y_i$ ) of the corners of the checkerboard were identified.

Registration was performed as described in the preceding section, and then  $P_{dst}$  was projected onto the mannequin's abdomen. The reprojection error between the actual checkerboard corners and reprojected corners was recorded using a digital caliper with accuracy to a tenth of a millimetre. This reprojection error is analogous to the reprojection error that would exist between the projected and actual vascular anatomy. 72 saddle points were measured as a sample of all the points that could be marked on the surface of the body form.

Next, five experiments were performed to determine the reprojection error as a function of the following experimental parameters:

*Projector\_height* - height of projector (m) above the surface of the mannequin, in metres

*Projector\_θ* - angle (degrees) between the vector that connects the umbilicus to the projector and a vector that is perpendicular to the coronal plane of the mannequin.

*Reg\_points\_dist* - average magnitude (cm) of the distance from each of the four registration points to the umbilicus.

*Mannequin\_#* - To simulate different body types two different mannequin models were used. One is a male mannequin and the other is a female mannequin. Figure 3 is a picture of mannequin #1.

The reprojection error is defined as the mean absolute error (in mm) of the distance between the actual checkerboard corners and projected checkerboard corners. The mean, standard deviation and maximum of the reprojection error for each experiment are reported.

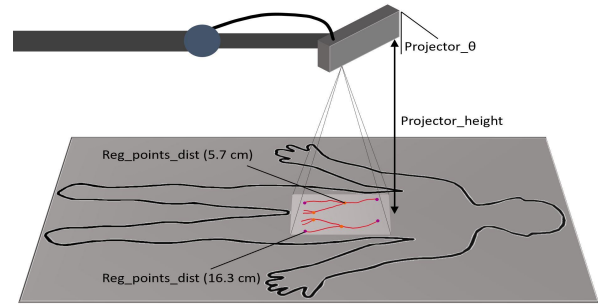


Figure 2: Diagram of experimental setup and parameters. The projector is mounted on a rigid arm and placed directly above the umbilicus of the patient/mannequin. The projector projects the distorted destination projector image ( $P_{dst}$ ).

III. RESULTS

The mean absolute reprojection error for the five experiments are shown in Table 1 below.

Table 1: Reprojection error as a function of several experimental parameters. Each column corresponds to an experiment.

	Experiment Number				
	1	2	3	4	5
<i>Projector_height</i> (m)	1.5	1.5	1.0	1.5	1.5
<i>Projector_θ</i> (°)	0	0	0	30	0
<i>Reg_points_dist</i> (cm)	5.7	16.3	16.3	16.3	16.3
<i>Mannequin_#</i>	1	1	1	1	2
<b>Mean Absolute Reprojection Error (mm)</b>	<b>3.0</b>	<b>1.7</b>	<b>1.7</b>	<b>4.3</b>	<b>1.7</b>
<b>Standard Deviation of Reprojection Error (mm)</b>	<b>1.8</b>	<b>1.0</b>	<b>1.1</b>	<b>2.7</b>	<b>1.0</b>
<b>Maximum of Reprojection Error (mm)</b>	<b>7.4</b>	<b>3.5</b>	<b>4.1</b>	<b>11.9</b>	<b>4.0</b>



Figure 3: Image of checkerboard saddle points projected onto the surgical mannequin. This provides a visual representation of the reprojection error.

#### IV. DISCUSSION AND FUTURE WORK

Analysis of the results in table 1 reveals that changing the parameters *Projector\_height* (*m*) and *Mannequin\_#* had little effect on the reprojection error. Whereas, increasing *Projector\_θ* ( $^{\circ}$ ) and decreasing *Reg\_points\_dist* (*cm*) resulted in increased reprojection error. Thus, two strategies for minimizing reprojection error are:

1) Minimize *Projector\_θ* ( $^{\circ}$ ) by placing the projector directly above the centerpoint of the virtual image ( $P_{src}$ ). In the current workflow that centerpoint is above the umbilicus.

2) Maximize *Reg\_points\_dist* (*cm*) by having the radiologist and surgeon both identify and mark four registration points that are at the extremes of the projector's field of view.

In general, the peripheral points had the largest reprojection error. Beyond that observation, there was no consistent spatial pattern for the reprojection error.

Collapsing the preoperative 3D segmented vascular anatomy into a 2D image ( $P_{src}$ ) significantly simplifies the preoperative to intraoperative registration and transformation. This simplification was justified because all patients, regardless of the amount of abdominal fat they have, all have underlying rectus muscles that are approximately planar. Furthermore, the surgeon will always remove the abdominal fat to expose the rectus muscle. More generally, the reprojection accuracy of 1.7mm is comparable to a previously reported reprojection error of 1.2 +/- 0.54mm for augmented reality projections of tumours during human brain surgery [8].

Future work will include using a brighter projector and quantifying the magnitude of intraoperative patient movement by video recording DIEP flap breast reconstruction surgeries with a camera that is held by a rigid arm one meter above the umbilicus of the patient. Next, in the clinical setting, the VascuLens reprojection error will be measured for DIE perforator arteries as they pierce through the rectus fascia. The comparative gold standards for artery perforator location will be both a Doppler ultrasound and direct surgeon visualization. Finally, a VascuLens system clinical trial for patients undergoing DIEP flap breast reconstruction surgeries will be conducted. The primary endpoints will be operative time and complication rates. Operative time saved may be up to 1-hour per operation.

An experimental ethics submission covering all of the future work described above has been made by one of the co-authors, Dr. Mike Stein, at Lenox Hill Hospital in New York, United States of America.

#### V. CONCLUSION

In conclusion, the VascuLens system is a novel proof-of-concept handsfree surgeon-in-the-loop augmented reality guidance system for DIEP flap breast reconstruction surgery. It has simple hardware, simple setup and intuitive user operation that only requires clicking on marks in the surgical field. Furthermore, the AR guidance is visible for all members of the surgical team, the accuracy is millimeter-level and the errors are well understood. These results are promising and provide significant motivation to make engineering improvements, do more validation and start clinical testing with the VascuLens system.

#### CONFLICT OF INTEREST AND ACKNOWLEDGEMENT

No conflict of interest to report. Funding for this research was provided by the 2020 Joule Innovation grant program and the BioTalent Student Work Placement Program.

#### REFERENCES

1. Lalla, R., Brown, T., & Griffiths, R. (2003). Where to draw the line: the error in marking surgical excision margins defined. *British Journal Of Plastic Surgery*, 56(6), 603-606.
2. Edgcumbe, Philip, Philip Pratt, Guang-Zhong Yang, Christopher Nguan, and Robert Rohling. "Pico lantern: Surface reconstruction and augmented reality in laparoscopic surgery using a pick-up laser projector." *Medical image analysis* 25, no. 1 (2015): 95-102.
3. Edgcumbe, Philip, Rohit Singla, Philip Pratt, Cait-lin Schneider, Christopher Nguan, and Robert Rohling. "Augmented reality imaging for robot-assisted partial nephrectomy surgery." In *International Conference on Medical Imaging and Augmented Reality*, pp. 139-150. Springer, Cham, 2016.
4. Pratt, P., Ives, M., Lawton, G., Simmons, J., Radev, N., Spyropoulou, L., & Amiras, D. (2018). Through the HoloLens™ looking glass: augmented reality for extremity reconstruction surgery using 3D vascular models with perforating vessels. *European Radiology Experimental*, 2(1).
5. Wesselius, Tycho S., Jene W. Meulstee, Gijs Luijten, Tong Xi, Thomas JJ Maal, and Dietmar JO Ulrich. "Holographic Augmented Reality for DIEP Flap Harvest." *Plastic and Reconstructive Surgery* 147, no. 1: 25e-29e.
6. Hummelink S, Hoogeveen YL, Schultze Kool LJ, Ulrich DJO. A New and Innovative Method of Preoperatively Planning and Projecting Vascular Anatomy in DIEP Flap Breast Reconstruction: A Randomized Controlled Trial. *Plast Reconstr Surg*. 2019 Jun;143(6):1151e-1158e.
7. Malowany, Kai Joseph, "Beyond Homographies: Exploration and Analysis of Image Warping for Projection in a Dome" (2017). Senior Projects Spring 2017. 315.
8. Tabrizi, L. B., & Mahvash, M. (2015). AR-guided neurosurgery: Accuracy and intraoperative application of an image projection technique. *J of Neurosurgery* 123(1), 206-211.